2052
doi:10.1017/S1431927619010997
Microsc. Microanal. 25 (Suppl 2), 2019

Identical Location STEM analysis on $La_{1-x}Sr_xCoO_3$ Oxygen-Evolution Catalysts

Xue Rui[1], Dongyoung Chung[2], Pietro Papa Lopes[2], Hong Zheng[2], John Mitchell[2], Nenad M. Markovic[2] and Robert Klie[1*]

[1.] Department of Physics, University of Illinois at Chicago, Chicago, IL, USA.
[2.] Materials Science Division, Argonne National Laboratory, Lemont, IL, USA.
* Corresponding author: rfklie@uic.edu

Oxygen evolution reaction (OER) is the key process for many energy storage applications, such as rechargeable metal-air battery. Good OER electro-catalysts, including metal oxide nanoparticles, should promote anionic redox of oxygen from water or hydroxide[1], but reactivity can originate from oxide material itself, both in bulk and at the particle surface.[2, 3] In perovskite oxides of the form ABO_3, it has been previously demonstrated that enhancing the hybridization between the O 2p and transition-metal *3d* orbitals can enhance the OER activity.[4] Doping the lanthanide *A*-site, as in Sr-doped $LaCoO_3$ (LSCO), has been widely utilized to affect the metal-oxygen covalence. With increasing the Sr^{2+} substitution of La^{3+}, the O *2p* band will move toward the Co *3d* band with decreasing Femi level, which can trigger the OER on lattice oxygen sites.[5] Meanwhile, Fe impurities in the KOH electrolyte have been found to significantly increase the activity of Ni-based perovskite oxide electrocatalysts.[6] Based on these results, we study the effects of Fe doping and Sr-doping in $LaCoO_3$-based electro-catalyst by establishing functional links between particle morphology (surface and bulk) and OER reactivity.

This contribution will utilize a combination of scanning transmission electron microscopy (STEM) imaging, electron energy loss spectrum (EELS) and energy dispersive x-ray (EDX) to examine the effects of electrochemical cycling of $La_{1-x}Sr_xCoO_3$ catalysts in an ultrapure KOH electrolyte and after the addition of trace levels of Fe. Specifically, we will compare the chemical composition, atomic structure and Co valence states of pristine and cycled samples. These studies are carried out in the JEOL-JEM ARM200CF equipped with Gatan Quantum Continuum spectrometer and Oxford X-max 100TLE windowless SDD X-ray detector.

Figure 1a) shows a pristine $LaCoO_3$ particle prior to any electro-catalytic cycling. After 50 electrochemical cycles in electrolyte, the formation of ordered oxygen vacancies was observed near the particle surface (Figure 1b). The addition of Fe to the KOH electrolyte results in the formation of additional ordered vacancies (Figure 1c), as well as the corrosion of the particle surfaces. It is important to point out here that all measurements are conducted on the identical particle throughout the electro-chemical cycling process.

For $La_{0.8}Sr_{0.2}CoO_3$ particles, we observe the stacking faults, similar to the Ruddlesden-Popper (RP) phase, formed within the particle and hexagonal La_2O_3 phase formed at the particle surface (Figure 2b) after electro-chemical cycling. In addition, we find CoO particle on the surface (as shown in Figure 2d), as well as non-uniform formation of various amorphous FeO(OH) and Fe_xO_y phases after the addition of Fe to the electrolyte (Figure 2e). Electron energy-loss spectroscopy is used to correlate the Co and Fe valence state to the concentration of oxygen vacancies and electro-chemical cycling conditions (Figures 2f and g). Finally, OER electro-chemical performance are correlated to oxygen vacancy and secondary phase formation to establish structure-activity-stability relationships on $LaSrCoO_3$ OER catalysts.

References:
[1] VR Stamenkovic et al., Nature Materials **16** (2016), p. 57.
[2] E Fabbri et al., Nature Materials **16** (2017), p. 925.
[3] X Cheng et al., Chemistry of Materials **27** (2015), p. 7662.
[4] JT Mefford et al., Nat Commun **7** (2016), p. 11053.
[5] A Grimaud et al., Nature Chemistry **9** (2017), p. 828.
[6] L Trotochaud et al., Journal of the American Chemical Society **136** (2014), p. 6744.
[7] This work is supported by National Science Foundation (No. DMR-1831406).

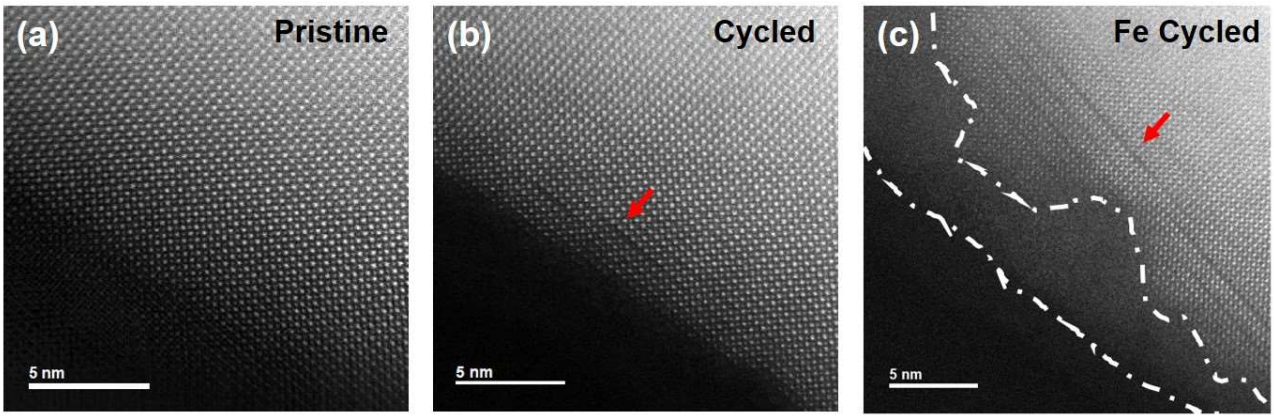

Figure 1. (a)-(c) HAADF image on pristine/cycled and iron cycled $LaCoO_3$ over the same region along the [1 0 0] direction. Oxygen vacancy ordering was marked on (b). More oxygen vacancy orderings and surface corrosion are marked in (c).

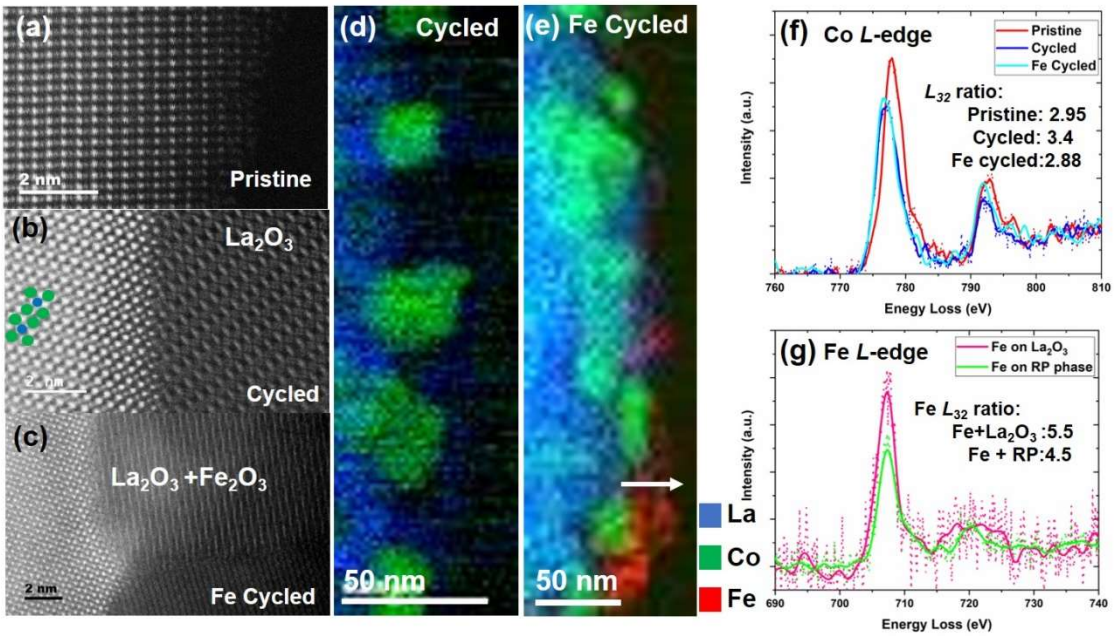

Figure 2. (a)-(c) HAADF image on pristine/cycled and Fe-cycled $La_{0.8}Sr_{0.2}CoO_3$ particle. This particle rotated by itself from [110] to [100] orientation after cycling. RP-phase in bulk part and La_2O_3 hexagonal phase on surface are marked in (b). (d)(e) Representative EELS element mapping on cycled and iron cycled $La_{0.8}Sr_{0.2}CoO_3$ particle. (f) Co L-edge spectrum recorded from pristine, cycled RP-phase region and Fe-cycled RP-phase with Fe region. (g) Fe L-edge spectrum extracted from Fe-cycled RP-phase and surface La_2O_3 region, as marked in (e).

https://doi.org/10.1017/S1431927619010997 Published online by Cambridge University Press